Korean J. of Chem. Eng., **14**(5), 312-320 (1997)

FACILITATED TRANSPORT OF CARBON DIOXIDE THROUGH AN IMMOBILIZED LIQUID MEMBRANE OF $K_2CO_3/KHCO_3$ AQUEOUS SOLUTION

Sang-Wook Park†, Nam-Hwan Heo*, Jeung-Seug Kim and Dong-Soo Suh

Department of Chem. Eng., Pusan National University, Pusan 609-735, Korea
*Technical Research Lab., POSCO., Pohang 790-600, Korea
(*Received 19 May 1997 • accepted 28 July 1997*)

Abstract – The facilitated transport of CO_2 through a hydrophilic polymeric membrane immobilized with K_2CO_3/$KHCO_3$ buffer solution has been investigated. The reactions of dissolved CO_2 in electrolyzed alkaline solution must consider hydration of CO_2 with water, chemical reaction of CO_2 with OH^- and dissociation of HCO_3^- into CO_3^{2-}. It is necessary to simplify these reactions as a simple model, which is used to analyze the transport system. From experiments in the liquid membrane with alkaline buffer solution, it is shown that the flux of CO_2 into $K_2CO_3/KHCO_3$ aqueous solution can be enhanced by the presence of CO_3^{2-}. A diffusion model with an overall reaction based on the film theory is proposed that predicts the experimentally observed facilitation factor with reasonable accuracy. The present model is compared with the rigorous diffusion model involving the complicated conventional chemical reactions.

Key words: Facilitated Transport, Alkaline Buffer Solution, CO_2, Film Theory Immobilized Liquid Membrane

INTRODUCTION

Separation of CO_2 is considered to be very important gas separation process [Kohl and Riesenfeld, 1985]. Recently, application of the membrane separation technique separating CO_2 has been the center of attention due to low energy consumption compared to traditional separation methods such as gas absorption and adsorption.

Membranes have been developed which make certain membrane separation processes economically and technically feasible since 1970's. Although several polymers such as silicone rubber and cellulose acetate are useful membrane materials, in general, polymer materials are not desirable as semipermeable membranes. Most polymer materials are relatively impermeable to all gases and liquids, and the separation factor of a permeate is low [Kesting and Fritzsche, 1993].

To overcome the problem of low selectivity, use of facilitated transport membrane has been proposed [Ward and Robb, 1967; LeBlanc et al., 1980]. Facilitated transport membranes containing carriers, which react reversibly and selectively with permeant species, has been attracting attention since they have much higher selectivity compared with polymer membranes without carriers [Kemena et al., 1983].

The most common reaction occurring in the carrier facilitated transport membrane is represented as

$$A+B \rightleftarrows AB$$

where, A is the component being transported across the membrane, B and AB represents the active chemical carriers, and the active carrier complex, respectively.

†To whom all correspondence should be addressed.

As the governing differential equations for this system are nonlinear due to reaction kinetics, a general analytical solution is not available. Many attempts have been made to obtain approximate solution of facilitation factor which is defined as the ratio of facilitated transport flux to the flux without carriers. Olander [1960] described simultaneous mass transfer combined with an equilibrium chemical reaction. Goddard et al. [1970] analyzed the behavior of facilitated transport membrane near chemical equilibrium condition. Friedlander and Keller [1965] used a linearized form of the reaction rate expression to describe the flux of permeate with reversible chemical reaction to the simple diffusional flux. Their assumptions were based on the reaction system being near equilibrium. Ward [1970], Smith et al. [1973] and Schultz et al. [1974] presented the two limiting conditions, reaction limited and diffusion limited. Chee et al. [1986] used the concept of a reaction boundary layer approximation to explain the physical problems with assuming instantaneous reaction equilibrium at the membrane boundary.

The chemical reactions of the dissolved carbon dioxide in the alkaline solutions are complicated by reactions of CO_2 with water and hydroxide ion, and dissociation of bicarbonate ion [Ward and Robb, 1967], therefore, it is necessary to simplify these complicated reaction for the optimal design of the immobilized membrane separator.

The purpose of this work is to propose a model that can handle the governing differential equations easily by means of simplifying the complicated chemical reactions to overall chemical reaction. The system of complicated chemical reactions carried out on this study is the $K_2CO_3/KHCO_3$ alkaline buffer aqueous solution, where is immobilized into pores of supporting membrane. The supporting membrane is a flat type of a microporous hydrophilic polymer membrane. The flux of CO_2 transported through the immobilized liquid membrane from gas mixture of CO_2 and N_2 is measured using an immobilized liquid membrane separator. The facilitated transport mechanism was analyzed from the comparison of experimentally measured values of facilitation factor of CO_2 with the theoretical values obtained from two models with the simplified and complicated chemical reactions, respectively.

THEORY

The total flux of CO_2 through an alkaline solution is the sum of the flux of physically dissolved CO_2, and that of HCO_3^- and CO_3^{2-} ions produced from the reactions [Ward and Robb, 1967]. In the $K_2CO_3/KHCO_3$ buffer solution, the several reactions take place:

$$CO_2+H_2O \rightleftarrows H^++HCO_3^- \tag{1}$$

$$CO_2+OH^- \rightleftarrows HCO_3^- \tag{2}$$

$$KHCO_3 \rightleftarrows K^++HCO_3^- \tag{3}$$

$$K_2CO_3 \rightleftarrows 2K^++CO_3^{2-} \tag{4}$$

$$H^++CO_3^{2-} \rightleftarrows HCO_3^- \tag{5}$$

$$H_2O \rightleftarrows H^++OH^- \tag{6}$$

The facilitated transport of CO_2 through the microporous polymeric membrane support immobilized with a alkaline solution can be described as following steps [Ward and Robb, 1967] :

(1) CO_2 is absorbed and dissolved at the high pressure side of the film.

(2) CO_3^{2-} obtained in aqueous solution reacts in alkaline solution to produce OH^- ion:

$$CO_3^{2-}+H_2O \longrightarrow HCO_3^-+OH^-$$

(3) The dissolved CO_2 reacts near the high pressure side of the liquid film:

$$CO_2+OH^- \longrightarrow HCO_3^-$$

(4) The produced HCO_3^- at the high pressure side is then diffused to the lower pressure side.

(5) The diffused HCO_3^- is dissociated at the lower pressure side:

$$HCO_3^- \longrightarrow OH^-+CO_2$$

$$HCO_3^- \longrightarrow H^++CO_3^{2-}$$

(6) The produced CO_2 in step (5) is released and separated.

(7) CO_3^{2-} ion in step (5) is then diffused again to the higher pressure side and the whole processes are repeated.

Therefore, CO_2, K_2CO_3, $KHCO_3$, HCO_3^-, CO_3^{2-}, H^+, OH^- and alkali metal (M) exist in the system under consideration.

At steady state, the material balance for each of the species can be expressed by the following form of equation,

$$D_i \frac{d^2 C_i}{dx^2} = R_i \tag{7}$$

The rate limiting reactions from (1) through (6) which occur in the aqueous alkaline solution are as follows [Kern, 1960],

$$CO_2 + H_2O \underset{k_{12}}{\overset{k_{11}}{\rightleftarrows}} H^+ + HCO_3^- \tag{8}$$

$$CO_2 + OH^- \underset{k_{22}}{\overset{k_{21}}{\rightleftarrows}} HCO_3^- \tag{9}$$

The resulting depletion rate expression of CO_2 is

$$R_A=(k_{11}+k_{21}[OH^-])\,[CO_2]-(k_{12}[H^+]+k_{22})\,[HCO_3^-] \tag{10}$$

The dissociation of water and HCO_3^- are sufficiently rapid, the equilibrium may be assumed,

$$K_w=[H^+]\,[OH^-] \tag{11}$$

$$K=\frac{[H^+][CO_3^{2-}]}{[HCO_3^-]} \tag{12}$$

At any point in liquid film, the condition of electrical neutrality is

$$[H^+]+[M^+]=[OH^-]+[HCO_3^-]+2[CO_3^{2-}] \tag{13}$$

Compared concentrations of H^+ and OH^- with the other ion concentrations, these are negligible. The above equation can then be simplified to

$$C_T=[M^+] \cong [HCO_3^-]+2[CO_3^{2-}] \tag{14}$$

The reaction rate equation and the mass balance of CO_2 can be derived from Eqs. (7) and (10) using Eqs. (11), (12) and (14):

$$D_A \frac{d^2 C_A}{dx^2}=R_A \tag{15}$$

$$R_A = k_{11} C_A - \frac{2K k_{12} C_E^2}{(C_T - C_E)} + \frac{K_w k_{21} C_A (C_T - C_E)}{2K C_E} - k_{22} C_E \tag{16}$$

The total material balance of carbon is

$$N_A^T=N_A+N_E+N_B \tag{17}$$

Since the concentration of metal ion in Eq. (14) is constant, the following equation can be obtained in liquid film:

$$\frac{dC_B}{dx} = -\frac{1}{2}\frac{dC_E}{dx} \tag{18}$$

If the diffusivities of HCO_3^- and CO_3^{2-} are equal, then

$$N_B = -\frac{1}{2} N_E \tag{19}$$

Substitution of Eq. (19) into Eq. (17) gives

$$D_A C_A + \frac{D_E}{2} C_E = a_1 x + a_2 \tag{20}$$

The governing equations can be derived in dimensionless form from Eqs. (15) and (20):

$$\frac{d^2\alpha}{d\eta^2}=m_1\alpha-m_2\frac{\beta^2}{(1-\beta)}+m_3\alpha\frac{(1-\beta)}{\beta}-m_4\beta \tag{21}$$

$$\alpha+p\beta=a_1'\eta+a_2' \tag{22}$$

where $\alpha=\frac{C_A}{C_{A0}},\ \beta=\frac{C_B}{C_T},\ \eta=\frac{x}{L},$

$$m_1=\frac{k_{11}L^2}{D_A},\ m_2=\frac{2Kk_{12}C_TL^2}{C_{A0}D_A},$$

$$m_3=\frac{k_{21}K_wL^2}{2KD_A},\ m_4=\frac{k_{22}C_TL^2}{C_{A0}D_A},$$

$$p=\frac{D_E C_T}{2D_A C_{A0}}, \tag{22a}$$

The boundary conditions of CO_2 are

$$\alpha(0)=1,\ \alpha(1)=\alpha_1 \tag{23}$$

Since HCO_3^- is a non-volatile species, the following boundary condition can be applied to the system:

$$\left.\frac{d\beta}{d\eta}\right|_0=\left.\frac{d\beta}{d\eta}\right|_1=0 \tag{24}$$

The diffusional mass transfer rate of CO_2 at high pressure side can be derived using the film theory as follows:

$$N_A^o=\frac{D_A}{L}(C_{A0}-C_{AL}) \tag{25}$$

The facilitation factor of CO_2 defined as ratio of N_A^T to N_A^o can be expressed as following dimensionless form,

$$\phi=\left.\frac{d\alpha}{d\eta}\right|_{\eta=0,1} \tag{26}$$

By adding up Eqs. (2), (5) and (6), the complicated reactions of CO_2 through several steps can be simplified to an overall reaction, a forward- and a backward-reaction represented by Eq. (27).

$$CO_2+CO_3^{2-}+H_2O \underset{k_2}{\overset{k_1}{\rightleftarrows}} 2HCO_3^- \tag{27}$$

The rate of reaction for CO_2 is

$$R_A=k_1\,C_A\,C_B-k_2\,C_E^2 \tag{28}$$

The following material balance of each component and boundary conditions can be derived from Eqs. (7) and (28):

$$D_A\frac{d^2C_A}{dx^2}=k_1\,C_A\,C_B-k_2\,C_E^2 \tag{29}$$

$$D_B\frac{d^2C_A}{dx^2}=k_1\,C_A\,C_B-k_2\,C_E^2 \tag{30}$$

$$D_E\frac{d^2C_E}{dx^2}=-k_1\,C_A\,C_B+k_2\,C_E^2 \tag{31}$$

$$x=0,\ C_A=C_{A0},\ \frac{dC_B}{dx}=\frac{dC_E}{dx}=0 \tag{32}$$

$$x=L,\ C_A=C_{AL},\ \frac{dC_B}{dx}=\frac{dC_E}{dx}=0 \tag{33}$$

The dimensionless forms of Eqs. (29) to (33) are

$$\frac{d^2\alpha}{d\eta^2}=m_5\,\alpha\,\beta+m_6\gamma^2 \tag{34}$$

$$\frac{d^2\beta}{d\eta^2}=m_7\,\alpha\,\beta+m_8\gamma^2 \tag{35}$$

$$\frac{d^2\gamma}{d\eta^2}=m_9\,\alpha\,\beta+m_{10}\gamma^2 \tag{36}$$

$$\alpha(0)=1,\ \left.\frac{d\beta}{d\eta}\right|_0=\left.\frac{d\gamma}{d\eta}\right|_0=0 \tag{37}$$

$$\alpha(1)=\alpha_1,\ \left.\frac{d\beta}{d\eta}\right|_1=\left.\frac{d\gamma}{d\eta}\right|_1=0 \tag{38}$$

where $m_5=\frac{k_1C_{B0}L^2}{D_A},\ m_6=-\frac{k_2C_T^2L^2}{C_{A0}D_A},$

$$m_7=\frac{k_1C_{A0}L^2}{D_B},\ m_8=-\frac{k_2C_TL^2}{D_B},$$

$$m_9=-\frac{k_1C_{A0}L^2}{D_E},\ m_{10}=\frac{k_2C_TL^2}{D_E},$$

$$\gamma=\frac{C_E}{C_T} \tag{38a}$$

EXPERIMENTAL

Chemicals in this study were reagent grade and used without further purification. The supporting membrane was a hydrophilic microporous cellulose acetate-nitrate membrane (AA-WP Type, 150 μm thick and 47 mm in diameter having an average pore size of 0.8 μm from Millipore Co.).

A schematic of the apparatus was shown in Fig. 1. The feed gas (mixture of N_2 and CO_2) and the sweep gas (N_2) were introduced through the upper and lower part of the gas permeation cell, respectively. The feed and sweep gases were humidified with distilled water to prevent the membrane drying, and their flow rates were controlled by a mass flow controller (Brooks Instrument Division Emerson Electric Co., 5850 Series).

Fig. 2 shows the detailed feature of the permeation cell. This cell was divided into up and downstream chamber by the microporous membrane and the perforated stainless steel plate (thickness of 0.2 cm). The permeation cell was sealed by a set of silicone rubber O-rings. The volume of up and downstream chambers are same, 4.4 cm^3, and diameter of the cir-

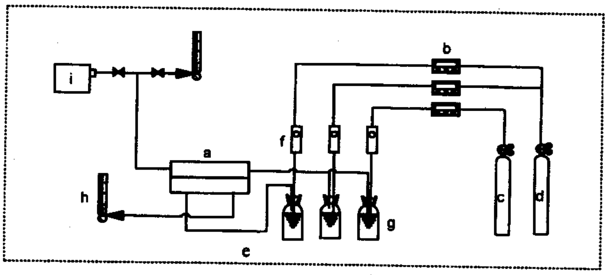

a. gas permeation cell d. N_2 cylinder g. saturation bottles
b. mass flow controller e. air chamber h. soap film meter
c. CO_2 cylinder f. rotameter i. gas chromatography

Fig. 1. Schematic diagram of experimental apparatus.

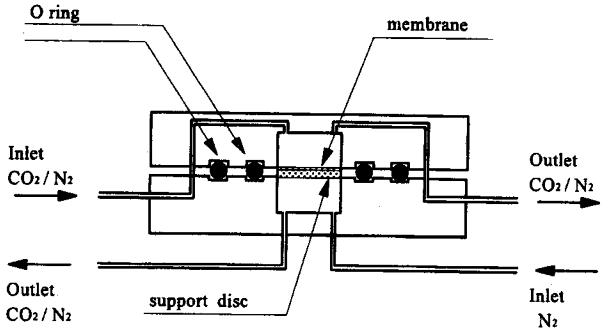

Fig. 2. Schematic diagram of permeation cell.

cular membrane exposed to gases is 4.4 cm.

The supporting membrane was immobilized with K_2CO_3/$KHCO_3$ buffer solution.

The feed and sweep gases were analyzed by gas chromatography (Shimadzu TCD GC-8A) with auto gas sampler and integrator (Shimadzu C-R6A Chromatopac). A Porapak Q (80/100 mesh) column was used for analyzing the permeated species in the gas streams. The diameter of stainless column was 1/8 inch and length of 6 feet. Temperatures of the oven and the injection port were 70 and 130 °C, respectively. The flow rate of carrier gas (He) was 20 cm^3/min.

The mass transport rates of CO_2 through the liquid film was determined by measuring the concentrations of CO_2 in inlet and outlet of the chambers at the steady state without change of outlet concentration of CO_2.

Experiments were carried out at 25 °C and 1 atm. The pressure of downstream chamber was regulated to 560 mmHg by a vacuum pump while the partial pressure of CO_2 in the upstream chamber was fixed at 0.2 atm. The concentration of K_2CO_3 in K_2CO_3/$KHCO_3$ solution were ranged of 0-0.5 mol/*l*. The buffer ratios, the concentration ratio of CO_3^{2-} to HCO_3^-, were varied 1, 5, and 10, by adding $KHCO_3$ to K_2CO_3 aqueous solution to maintain the buffer ratio according to the following reaction,

$$CO_3^{2-} + H_2O \overset{K_b}{\rightleftarrows} HCO_3^- + OH^- \tag{39}$$

The equilibrium constant (K_b) for reaction (39) at 25 °C is 2.15×10^{-4} mole/*l* [Danckwerts and Sharma, 1966].

RESULTS AND DISCUSSION

1. Measurements and Estimations of Physical Properties

To determine the mass transfer rate of CO_2 experimentally and theoretically, we have founded the physical properties of diffusivity, solubility and chemical reaction constants which are effected by the ionic strength of K_2CO_3/$KHCO_3$ buffer solution and the concentrations of HCO_3^-, CO_3^{2-} and OH^-.

1-1. Solubility of CO_2

The solubility of CO_2 in the dilute electrolyte solutions at 25 °C and 1 atm can be estimated by the method of van Krevelen and Hoftijzer [Danckwerts, 1970].

$$\log\left(\frac{H}{H^o}\right) = hI \tag{40}$$

where H^o is the Henry constant in water given in the literature [Danckwerts, 1970], h is the salting-out parameter referring to the species of ions present in electrolyte solution and to the species of gas. I is the ionic strength of the solution defined by

$$I = \frac{1}{2}\sum_{i=0}^{n} C_i z_i^2 \tag{41}$$

Where C_i is the concentration of component i having the valency z_i. The quantity h in Eq. (40) is the sum of contributions referring to the species of positive and negative ions and to the species of gas:

$$h = h_+ + h_- + h_G \tag{42}$$

For the CO_2 absorption into the alkaline solution, h_+, h_- and h_G are 0.074, 0.021, −0.019 *l*/g-ion, respectively [Danckwerts, 1970].

1-2. Diffusivity

Diffusivity of CO_2 in K_2CO_3/$KHCO_3$ buffer solutions at 25 °C and 1 atm is calculated by the modified equation from the correlation of Hikita et al. [1976].

$$\frac{D_A}{D_{AO}} = 1 - (\xi_1[CO_3^{2-}] + \xi_2[HCO_3^-] + \xi_3[OH^-]) \tag{43}$$

Where ξ_1, ξ_2 and ξ_3 are the correlation constants having the values of 0.261, 0.140 and 0.129 *l*/mol, respectively. D_{AO} is diffusivity of CO_2 in water and has the value of 1.97×10^{-5} cm^2/s [Hikita et al., 1976]. It is assumed that the ratios of diffusivity of CO_3^{2-} and HCO_3^- to the diffusivity of CO_2 are equal to those in the infinite dilute solution. D_B/D_A and D_E/D_A are 0.51 and 0.56, respectively [Hikita et al., 1976].

1-3. Reaction Rate Constants

The reaction rate constant k_{11} is 0.0375 s^{-1} [Kern, 1960] and k_{21} is calculated from the following equation proposed by Pinsent et al. [1956],

$$\log k_{21} = \log k_{21}^0 + 0.20\, I - 0.0182\, I^2 \tag{44}$$

$$\log k_{21}^0 = 13.635 - 2895/T \tag{45}$$

k_{12} and k_{22} is 5.5×10^4 *l*/mol · s and 2×10^{-4} s^{-1} in the literature of Gibbons and Edsall [1963], respectively.

The reaction between CO_2 and alkaline buffer solution such as Eq. (27) falls in a slow reaction regime [Doraiswany and Sharma, 1984]. The following equations hold for this case,

$$N_A\, a = k_1 A_0 B_0 = k_L\, a\, (A^* - A_0) \tag{46}$$

Eq. (46) can be solved to give

$$\frac{A^*}{N_A a} = \frac{1}{k_L a} + \frac{1}{k_1 B_0} \tag{47}$$

where, B_0 is the concentration of OH^- in the alkaline buffer solution, and it can be calculated from the following equation using Eq. (39) [Danckwerts and Sharma, 1966].

$$B_0 = K_b \frac{[CO_3^{2-}]}{[HCO_3^-]} \tag{48}$$

The forward reaction rate constant (k_1) can be obtained from the measured mass transfer rate of CO_2 at the given concen-

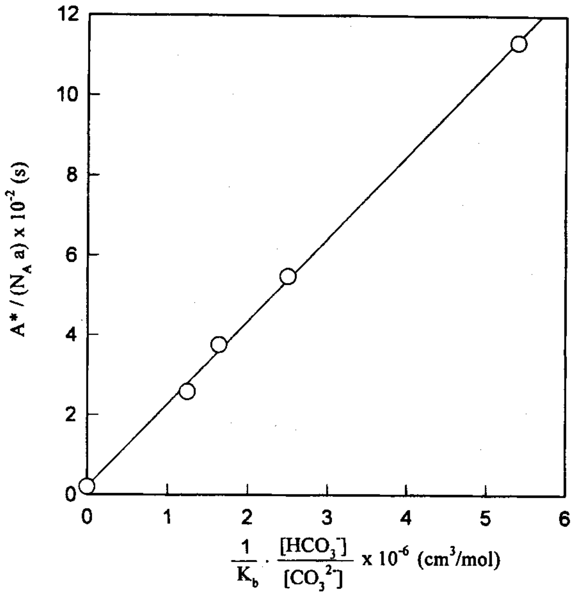

Fig. 3. Dependence of concentration of K_2CO_3 on the absorption rate of CO_2 into $K_2CO_3/KHCO_3$ aqueous buffer solution.

tration of K_2CO_3 and buffer ratio using Eqs. (47) and (48).

The mass transfer rates of CO_2 were measured in a flat agitator used in the previous study [Park et al., 1995] in the range of K_2CO_3 from 0.1 to 0.5 mol/*l* and the buffer ratio, 1, and the results are shown in Fig. 3. The plot of A^*/N_A a against $[HCO_3^-]/K_b[CO_3^{2-}]$ is a straight line from the experimental data as shown in Fig. 3. The forward reaction rate constant (k_1) could be obtained from the slope of this straight line, and it is 4.9 *l*/mol · s at 25 °C. The equilibrium constant Eq. (27) were 7.7×10^3 at 25 °C from the literature [Ward and Robb, 1967].

The backward reaction rate constant (k_2) was calculated as 6.4×10^{4} *l*/mol · s from k_1 and the equilibrium constant.

1-4. Measurement of Tortuosity of Liquid Membrane

To measure the tortuosity of hydrophilic microporous membrane, the flux of CO_2 through the membrane immobilized with water was measured with the changes of the partial pressure of CO_2 at inlet of high pressure side in the permeation cell. The flow rates of feed and sweep gas were 40 and 20 cm^3/min, respectively. A plot of the permeation rate of CO_2 versus the partial pressure difference of CO_2 between the high and low pressure side is shown in Fig. 4. In this figure, the plots have a linear relationship with the slope of 1.508×10^{-8} mol/cm^2 · s · atm. The thickness of liquid membrane is calculated by the slope obtained in Fig. 4 and Eq. (49) derived from Fick's law, and the value is 0.0457 cm. As nominal thickness of the polymer membrane used in this work is 0.015 cm, the tortuosity defined as the ratio of L to the nominal thickness is 3.05.

$$N_A^o = \frac{D_{A0}}{H^o L}\Delta P \qquad (49)$$

2. Effects of the Experimental Variables on CO_2 Permeation Rate

The mass transfer rate of CO_2 without chemical reaction

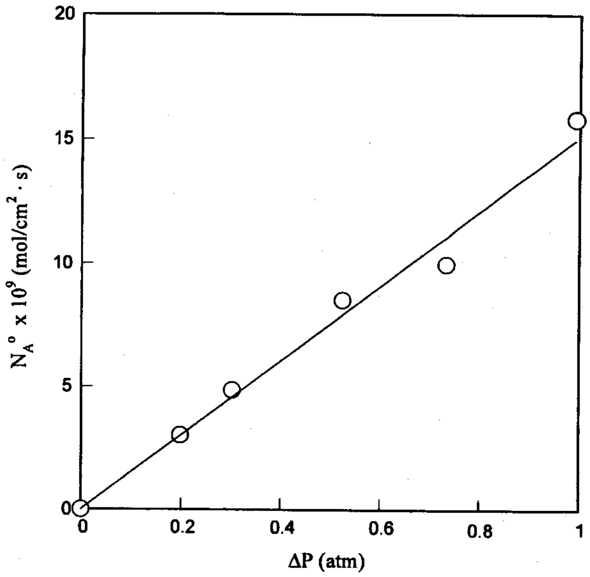

Fig. 4. Effect of ΔP on the flux of CO_2 with H_2O as a carrier.

should be measured to determine the facilitation factor of CO_2 in $K_2CO_3/KHCO_3$ buffer solution. The mass transfer rate of CO_2 was measured through the NaCl electrolyte solution having the same ionic strength as a given concentration of $K_2CO_3/KHCO_3$ solution. The flow rate of feed gas is 40 cm^3/min having the partial pressure of 0.2 atm. Fig. 5 shows the effect of ionic strength of the buffer solution on the permeation rate of CO_2 when buffer ratio was 1. The ionic strength corresponding to the buffer solution was adjusted by NaCl solution. In this figure, the calculated values from Eq. (25) were also plotted as solid line. The solubility of CO_2 was decreased with the ionic strength of solution, then the value of N_A^o is decreased with increasing the concentration of NaCl. The experimental results were well agreed with the calculated ones from Eq. (25).

The concentrations of CO_2, HCO_3^- and CO_3^{2-} were ob-

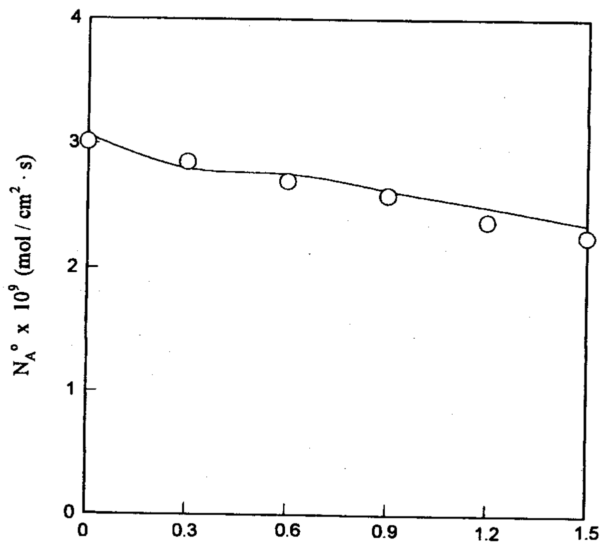

Fig. 5. Effect of ionic strength on mass transfer rate of CO_2.

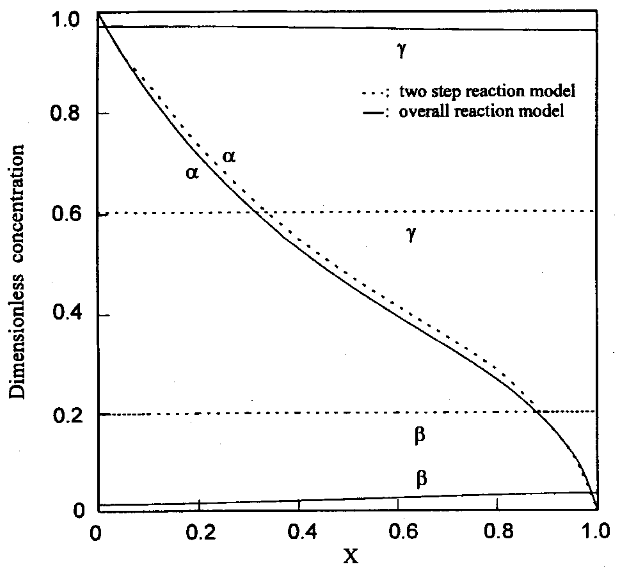

Fig. 6. Dimensionless concentration profile in the immobilized K_2CO_3 aqueous solution.
(CO_3^{2-}/HCO_3^-=1, [K_2CO_3]=0.3 mol/l)

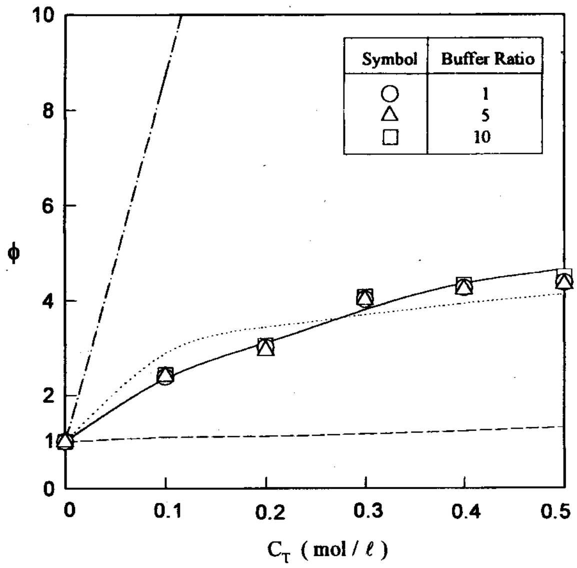

Fig. 7. Effect of carrier concentration on facilitation factor.
(···: two step reaction model, —: overall reaction model, -·-: fast reaction, - -: slow reaction)

tained from numerical solutions of mass balance Eq. (21), (22) with reactions (8) and (9) (hereafter two-step reaction model), and (34)-(36) with reaction (27) (overall reaction model) by successive approximation technique.

Fig. 6 shows typical concentration profile of CO_2, CO_3^{2-} and HCO_3^- as dimensionless forms like α, β and γ in the membrane for the case of partial pressure of CO_2, 0.2 atm, concentration of K_2CO_3, 0.3 mol/l, and buffer ratio, 1. The solid lines represent the concentration profile calculated from the overall reaction model and the dotted lines those from two-step reaction model. These two concentration profiles are different from each other especially in the middle part of the membrane. In spite of such a large difference between the two concentration profiles, numerically obtained facilitation factor by overall reaction model, i.e., 3.78, is closed to that obtained by two-step reaction model, 3.70. This suggests that profile of the overall reaction model agrees with profile of the two-step reaction model near the feed side interface. This behavior is indeed clearly seen in the figure as can be expected from the nature of the present overall reaction model, i.e., the reaction of CO_2 in K_2CO_3/$KHCO_3$ buffer solution acts as the overall reaction such as Eq. (27).

The facilitation factor of CO_2 were calculated numerically in the range of the concentration of K_2CO_3 from 0.1 to 0.5 mol/l. The results are shown in Fig. 7 for the buffer ratios of 1, 5 and 10. In this figure, the facilitation factor of CO_2 increases as initial concentration of K_2CO_3 increases. This is caused by the increase of OH^- concentration as increase of initial concentration of K_2CO_3 by Eq. (39). However, the facilitation factor of CO_2 is not affected by the buffer ratio. This result is agreed with the previous work [Hikita et al., 1976] analyzed the absorption of CO_2 as the step reactions (8) and (9) in the CO_3^{2-}/HCO_3^- buffer solution.

Analytical solutions for two limiting cases are available. One is the diffusion-rate limited case, and the other is reaction-rate limited. If the rate of overall reaction in Eq. (27) is very fast, the reversibility of reaction exists throughout the membrane. Adding Eq. (29) to Eq. (31), the following equation is derived.

$$D_A \frac{d^2 C_A}{dx^2} + D_E \frac{d^2 C_E}{dx^2} = 0 \tag{50}$$

The solution of Eq. (50) is

$$D_A C_A + D_E C_E = a_1'' x + a_2'' \tag{51}$$

where a_1'' and a_2'' are constants. The overall mass transfer rate of CO_2 for the diffusion-rate limited is defined as follows,

$$N_{fast} = -D_A \frac{dC_A}{dx} - D_E \frac{dC_E}{dx} \tag{52}$$

Because Eq. (52) can be applied throughout the whole region of the membrane, as equilibrium state between CO_2 and HCO_3^-, N_{fast} is denoted as follows,

$$N_{fast} = \frac{D_A}{L}(C_{A0} - C_{AL}) + \frac{D_E}{L} K_{eq} (C_{A0} - C_{AL}) \tag{53}$$

In this case, the facilitation factor, ϕ_{fast}, is available from Eqs. (25) and (53).

On the other hand, if the rate of overall reaction in Eq. (27) is very slow, C_B and C_E remain constant as $\overline{C}_B$, $\overline{C}_E$, respectively. The analytical solution can be obtained from Eq. (29) by replacing C_B and C_E as $\overline{C}_B$ and $\overline{C}_E$, respectively as follows,

$$C_A = \frac{B_1}{k_1} \sinh(\sqrt{k_1/D_A}\, x) + \frac{B_2}{k_1} \cosh(\sqrt{k_1/D_A}\, x) + \frac{k_2 \overline{C}_E}{k_1} \tag{54}$$

where, $\overline{C}_E = \frac{k_1(C_{A0} + C_{AL})}{2k_2}$,

$$B_1 = \frac{k_1 C_{AL} - k_2 \overline{C}_E - B_2 \cosh\sqrt{(k_1/D_A)}L}{\sinh\sqrt{(k_1/D_A)}L}, \quad B_2 = k_1 C_{A0} - k_2 \overline{C}_E$$

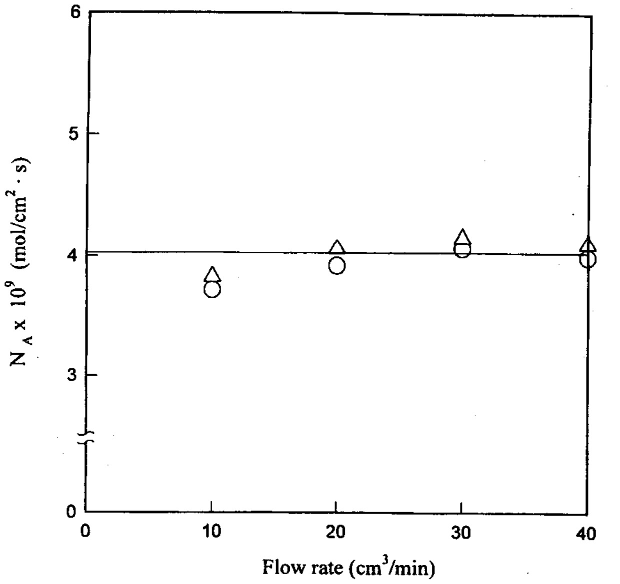

Fig. 8. Effect of upstream and downstream flow rate on the flux of CO_2.
(○: upstream flow rate, △: downstrean flow rate, —: numerical value).

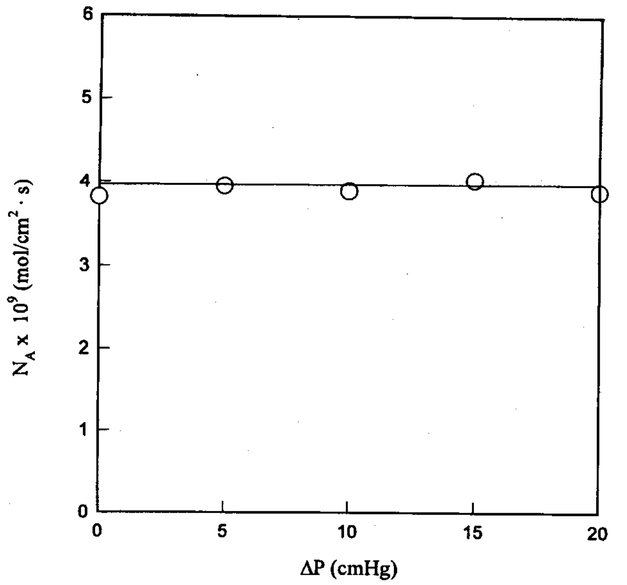

Fig. 9. Effect of pressure difference between upstream and downstream on the flux of CO_2.
(—: numerical value)

The mass transfer rate of CO_2 in the case of reaction-rate limited is derived from the concentration gradient of Eq. (54) and is expressed as follows,

$$N_{slow} = -D_A \frac{B_1\sqrt{k_1/D_A}}{k_1} \tag{55}$$

The facilitation factor in this case of, ϕ_{slow}, can be obtained from Eqs. (25) and (55).

The facilitation factors for two limiting cases are also represented in Fig. 7 as a function of the initial concentration of K_2CO_3 in the liquid membrane. Comparing the facilitation factors for two limiting cases with the experimental values is shown in Fig. 7. The experimental values were closer to those of reaction-rate limited. Thus, this implies that the facilitated transport of CO_2 in $K_2CO_3/KHCO_3$ buffer solution can be analyzed in terms of slow reaction, and this is agreed with the previous work [Ward and Robb, 1967].

The mass transfer rates of CO_2 were measured in the range of feed- and sweep-gas flow rate from 10 to 40 cm^3/min. Fig. 8 shows the experimental fluxes of CO_2 for the concentration of K_2CO_3, 0.2 mol/*l* and buffer ratio 1. The solid line represents the numerical value for the overall reaction model. The mass transfer rate of CO_2 was held constant to the change of feed-gas or sweep-gas flow rate. The effects of the pressure difference between up- and downstream on the permeation of CO_2 were also tested for the concentration of K_2CO_3, 0.2 mol/*l* and buffer ratio 1. The measured mass transfer rate of versus the pressure difference are shown in Fig. 9 in the range of the pressure of downstream from 760 to 560 mmHg with fixing total pressure and partial pressure of CO_2 in upstream to 1 and 0.2 atm. The solid line represents the theoretical value for overall reaction model. It is confirmed that the immobilized liquid membrane is stable because it was not affected by the flow rate and the pressure difference of gas outside the membrane, as shown in Fig. 8 and 9.

The mass transfer rates of CO_2 were measured in the range of partial pressure of CO_2 in the feed gas from 0.1 to 0.5 atm for K_2CO_3 concentration, 0.3 mol/*l*, buffer ratio, 1, and flow rate of upsteam, 40 cm^3/min, and is shown in Fig. 10.

The solid line represents the numerical value for the overall reaction model. As shown in Fig. 10, the fluxes of CO_2 increased as the partial pressure of CO_2 increased. This is due to the increase of solubility of CO_2 by the increase of

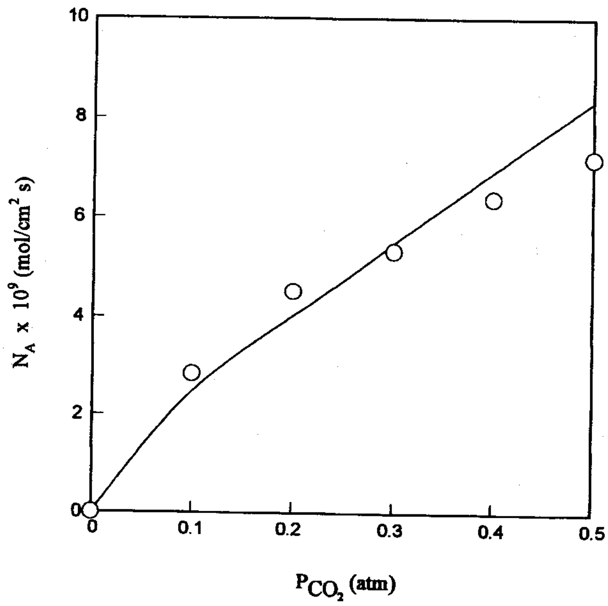

Fig. 10. Effect of P_{CO_2} on the flux of CO_2 in upstream.
(—: numerical value).

partial pressure of CO_2, but it was noted that some deviation between the experimental and the numerical values occurred above 0.3 atm of partial pressure of CO_2. This is because the estimation method such as Eq. (40) used in this study for the solubility of CO_2 can be valid only in the case of the dilute electrolyte solution.

CONCLUSION

The mass transfer rates of CO_2 through the reactive liquid membrane supported with a hydrophilic microporous polymeric membrane immobilized with aqueous $K_2CO_3/KHCO_3$ buffer solution were measured at an atmospheric pressure and room temperature by varying the flowrates of CO_2 from 10 to 40 cm^3/min, the concentration of K_2CO_3 from 0 to 0.5 mol/*l* and buffer ratio of 1, 5, 10.

The mass transfer rate of CO_2 through the buffer solution is analyzed from a diffusion model with simplifying the reaction of CO_2 as an overall reaction. Reaction is first order respect to CO_2 and CO_3^{2-} in forward reaction and 2nd-order with HCO_3^- in backward reaction. Comparing this model to the conventional diffusion model including the hydration reaction with CO_2 and the reaction of CO_2 with OH^- ion, it can be used for the analysis of the facilitated transport of CO_2 through the buffer solution. The measured flux of CO_2 was close to the numerical value based on the overall reaction model.

The measured mass transfer rates of CO_2 were increased as K_2CO_3 concentration and partial pressure of CO_2 increased, respectively, and held constant to the change of the buffer ratios. The reaction of CO_2 in buffer solution was found to fall within the slow reaction region. The stability of liquid membrane immobilized within the microporous polymeric support was confirmed by the experimental results without significant changes of gas flowrate and pressure.

ACKNOWLEDGEMENT

This paper was supported by special fund for UNIVERSITY RESEARCH INSTITUTE, Korea Research Education.

NOMENCLATURE

a : interface area of gas and liquid [cm^2/cm^3]
a_1, a_2, a_1', a_2', a_1'', a_2'' : integration constants in Eq. (20), (22) and (51), respectively
A* : concentration of CO_2 in the buffer solution at gas-liquid interface [mol/cm^3]
A_0 : concentration of CO_2 in the bulk body of the buffer solution [mol/cm^3]
B_0 : concentration of OH^- in the buffer solution [mol/cm^3]
C_{A0}, C_{AL} : concentration of CO_2 in the membrane at upstream and downstream, respectively [mol/cm^3]
C_A : concentration of CO_2 [mol/cm^3]
C_B : concentration of CO_3^{2-} [mol/cm^3]
C_E : concentration of HCO_3^- [mol/cm^3]
C_i : concentration of species i [mol/cm^3]
C_T : total concentration of carbonate and bicarbonate [mol/cm^3]
D_i : diffusion coefficient of species i [cm^2/sec]
h : salting-out parameter [*l*/g-ion]
H : Henry's constant [mol/cm^3 · atm]
H_0 : Henry's constant of H_2O [mol/cm^3 · atm]
i : species i
I : ionic strength [g-ion/*l*]
k_1, k_2: forward and backward reaction rate constant defined by reaction (27) [sec^{-1}]
k_{11}, k_{21} : forward reaction rate constant defined by reactions (8) and (9), respectively [sec^{-1}], [cm^3/mol · sec]
k_{21}, k_{22} : backward reaction rate constant defined by reactions (8) and (9), respectively [cm^3/mol · sec], [sec^{-1}]
K : second ionization constant for H_2CO_3 defined by Eq. (12) [mol/cm^3]
K_1 : equilibrium constant of reaction (27)
K_b : equilibrium constant of reaction (39) [mol/cm^3]
K_w : dissociation constant of water [mol/cm^3]^2
L : film thickness [cm]
M : alkaline metal
N_i : flux of species i [mol/cm^2 · sec]
N_i^T : total flux of species i [mol/cm^2 · sec]
N_i^0 : flux without chemical reaction of species i [mol/cm^2 · sec]
N_{fast} : flux of CO_2 in fast reaction [mol/cm^2 · sec]
N_{slow} : flux of CO_2 in slow reaction [mol/cm^2 · sec]
ΔP : pressure difference between upsteam and downstream [atm]
R_i : reaction rate of i component [mol/cm^3 · sec]
T : temperature [K]
x : coordinate axis
z_i : valency of ions

Greek Letters

α, β, γ : dimensionless concentration of CO_2, CO_3^{2-} and HCO_3^-, respectively
η : dimensionless distance
ζ_i : correlation constant of i component [*l*/mol]
ϕ : facilitation factor

REFERENCES

Chee, Y. C., Jung, Y. W. and Ihm, S. K., "Parameter Effects on the Facilitated Transport of Carbon Dioxide", *HWAHAK KONGHAK*, **24**, 227 (1986).

Danckwerts, P. V. and Sharma, M. M., "The Absorption of Carbon Dioxide into Solutions of Alkalis and Amines", *Chem. Eng.*, CE244 (1966).

Danckwerts, P. V., "Gas-Liquid Reactions", McGraw-Hill Book Company (1970).

Doraiswany, L. K. and Sharma, M. M., "Heterogeneous Reaction: Analysis, Examples and Reactor Design", volume 2, John Wiley & Sons, New York, **2**, 19 (1984).

Friedlander, S. K. and Keller, K. H., "Mass Transfer in Reacting System near Equilibrium", *Chem. Eng. Sci.*, **20**, 121 (1965).

Gibbons, B. H. and Edsall, J. T., "Rate of Hydration of Carbon Dioxide and Dehydration of Carbonic Acid at 25 °C", *J. Biol. Chem.*, **238**, 3502 (1963).

Goddard, J. D., Schultz, J. S. and Bassett, R. J., "On Membrane Diffusion with near-Equilibrium Reaction", *Chem.*

Eng. Sci., **25**, 665 (1970).
Hikita, H., Asai, S. and Takatsuka, T., "Absorption of Carbon Dioxide into Aqueous Sodium Hydroxide and Sodium Carbonate-Bicarbonate Solutions", *Chem. Eng. J.*, **11**, 131 (1976).
Kemena, L. L., Noble, R. D. and Kemp, N. J., "Optimal Regimes of Facilitated Transport", *J. Mem. Sci.*, **15**, 259 (1983).
Kern, D. M., "The Hydration of Carbon Dioxide", *J. Chem. Educ.*, **37**, 14 (1960).
Kesting, R. E. and Fritzsche, A. K., "Polymer Gas Separation Membrane", John Wiley & Sons (1993).
Kohl, A. L. and Riesenfeld, F. C., "Gas Purification", Gulf Publishing Co. (1985).
LeBlanc, O. H., Ward, W. J. and Matson, S. L., "Facilitated Transport in Ion-Exchange Membrane", *J. Mem. Sci.*, **6**, 339 (1980).
Olander, D. R., "Simultaneous Mass Transfer and Equilibrium Chemical Reaction", *AIChE J.*, **6**, 233 (1960).
Park, S. W., Park, D. W., Suh, D. S. and Heo, N. H., "Oxidation of Diphenylmethane by O_2 Gas with Tetrabutylammonium Hydrogen Sulfate", *HWAHAK KONGHAK*, **33**, 318 (1995).
Pinsent, B. R. W., Peason, L. and Roughton, F. J. W., "The Kinetics of Combination of Carbon Dioxide with Hydroxide Ions", *Trans. Faraday Soc.*, **52**, 1512 (1956).
Smith, K. A., Meldon, J. H. and Colton, C. K., "An Analysis of Carrier-Facilitated Transport", *AIChE J.*, **19**, 102 (1973).
Schultz, J. S., Goddard, J. D. and Suchdeo, S. R., "Facilitated Transport via Carrier-Mediated Diffusion in Membranes", *AIChE J.*, **20**, 417 (1974).
Ward, W. J. and Robb, W. L., "Carbon Dioxide-Oxygen Separation: Facilitated Transport of Carbon Dioxide Across a Liquid Film", *Science*, **156**, 1481 (1967).
Ward, W. J., "Analytical and Experimental Studies of Facilitated Transport", *AIChE J.*, **16**, 405 (1970).